J Supercond Nov Magn (2015) 28:1501–1506
DOI 10.1007/s10948-014-2942-0

ORIGINAL PAPER

A Significant Enhancement in J_c Values Through Excessive Na Doping in $Bi_2Sr_2Ca_1Cu_{2-x}Na_xO_y$ Superconductors

Berdan Özkurt

Received: 14 November 2014 / Accepted: 16 December 2014 / Published online: 28 December 2014

Abstract In this study, the effects of excessive Na substitution on the structural and physical properties of $Bi_2Sr_2Ca_1Cu_{2-x}Na_xO_y$ samples with $x = 0.3$, 0.35, 0.4, and 0.5 prepared by a conventional solid-state reaction method were investigated by means of X-ray powder diffraction (XRD), scanning electron microscope (SEM), DC electrical resistivity, and magnetic hysteresis loop measurements. It is observed from SEM images that the granular nature of Bi-2212 phase improves significantly for sample containing maximum $x = 0.5$ Na content in this work. Bean's critical state model is used to determine the field dependence of critical current density (J_c) from the M-H curves for all samples. It is found that the sample including $x = 0.5$ Na content has the highest J_c values due to the improved superconducting properties with its more granular microstructure.

Keywords High-T_c superconductors · XRD · Magnetic hysteresis loop · Critical current density

1 Introduction

For important technological applications, BSCCO system including high-temperature phases such as Bi-(2212) and Bi-(2223) still needs to possess better magnetic field carrying capacity (H_c) and higher critical current density (J_c). While it is very difficult to reach high J_c values in the presence of high magnetic fields in BSCCO ceramics, higher J_c and H_c values can be obtained as based on enhancements in their flux pinning properties. It is well known that mixed state in type II superconductors includes the vortex motions causing the flux-flow resistance. Defects such as both point and line which can act as effective pinning centers are necessary to pin the motion of vortex. It is obvious that impurities doped into BSCCO system can create such useful defects, implying the enhancement of the superconducting properties of the BSCCO system due to improvements in the number of the flux pinning centers.

Thus, one of the most widely used methods to improve J_c values of BSCCO ceramics has been the substitution or addition of metallic elements having different ionic radii and electronic configuration such as Li, Nb, B, Cd, Sn, Ag, and Pb [1–13]. Especially, the flux pinning capability of the ceramic superconductors can be significantly increased when these doping elements cause point-like defects which ensure to pin the magnetic flux in crystallographic structure with the adding of foreign particles such as NiO in BSCCO system due to the formation of large point-like defects [14–17]. On the other hand, it is generally believed that doping to Cu site is not suggestible because it includes layers related to superconducting in the unit cell of ceramic superconductors. However, some studies confirmed that the substitution of Na for Cu site into BSCCO ceramics increases significantly the intergranular critical current density (J_c) and remnant magnetization (M_R) values due to large grain thickness occurred by probably reducing the phase formation temperature. Moreover, there are also a lot of studies on the useful effects of Na doping on the superconducting and mechanical properties of BSCCO ceramics [18–20].

In addition, another important factor to increase J_c and H_c values is to have bigger grain size and more regular

B. Özkurt (✉)
Department of Energy Systems Engineering,
University of Mersin, 33400 Mersin, Turkey
e-mail: berdanozkurt@mersin.edu.tr

grain connectivity in the structure. It is well known that the J_c values strongly depend on the orientation, size, and thickness of grains.

Such improvements in the size of grains can be expected as depending on the formation of a liquid phase started in lower temperatures from their crystallization temperature without decomposition of the high-temperature phases such as Bi-2212 and Bi-2223 into non-superconducting phases. On the other hand, voids and porosity occurred by melting some Bi atoms due to long calcination process in the microstructures of ceramic superconductors in a high-temperature furnace can cause severe problems in grain connectivity, destroying the electricity transmission without losses.

In the previous work, the influence of Na substitution on superconducting properties of BSCCO ceramics produced using the conventional solid-state reaction technique was investigated, indicating that $Bi_2Sr_2Ca_1Cu_{1.75}Na_{0.25}O_y$ sample including $x = 0.25$ Na content has the largest hysteresis curve and the largest grain size. These results reveal that Na substitution is necessary for the enhancements in grain connectivity together with less porosity.

In this paper, the structural and physical properties of excess sodium doped $Bi_2Sr_2Ca_1Cu_{2-x}Na_xO_y$ in the concentration range of $x = 0.3 - 0.5$ for Cu sites in Bi-2212 phase are investigated to find the best stoichiometric amounts of Na. The prepared samples have been characterized by using X-ray powder diffraction (XRD), SEM, electrical resistivity, and magnetic measurements.

2 Experimental

Polycrystalline samples of $Bi_2Sr_2Ca_1Cu_{2-x}Na_xO_y$ with $x = 0.3$, 0.35, 0.4, and 0.5 were prepared by the standard solid-state reaction methods and labeled as N5, N6, N7, and N8, respectively. High-purity powders of commercial Bi_2O_3 (Aldrich, 99 %), $SrCO_3$ (Alfa Aesar, 99.99 %), $CaCO_3$ (Aldrich, 99.9 %), CuO (Aldrich, 99.99 %), and Na_2CO_3 (Aldrich, 99 %) in the preparation of Bi-2212 ceramic samples were used. They were weighed in the appropriate proportions, mixed, and milled. After the milling process, the homogenous mixture of powders was pressed into pellets of 1.3 cm in diameter by applying a 375-MPa pressure and calcined at 750 °C for 12 h. The calcined pellets were reground, repressed, and recalcined twice at 820 °C for 24 h to start the formation of the superconducting phase.

Finally, precursor materials were ground and repressed and annealed at 845 °C for 120 h in order to reach a large amount of pure 2212-BSCCO.

Resistivity and magnetic measurements were carried out on the samples using Cryogenic Limited PPMS (from 5 to 300 K) which can reach the cryogenic temperatures of about to 2 K in a closed-loop He system. X-ray powder diffraction analyses to determine the phases present in the samples were performed by using a Rigaku Ultima IV X-Ray Diffractometer with a constant scan rate (2°/min) in the range of $2\theta = 3°$–$60°$. Lattice parameters have been automatically calculated by the PDXL software version 1.6.0.1 with the ICDD version 6.0 database. The surface morphologies of the samples were studied by using a Zeiss/Supra 55 Scanning Electron Microscope (SEM).

Table 1 Lattice parameters and resistivity measurement results for the samples

Samples	a (Å)	b (Å)	c (Å)	T_C^{onset} (K)	T_C^{offset} (K)	mΩ cm at 300 K
N5	3.813	3.813	30.807	78.2	62.1	2.32
N6	5.406	5.399	30.833	76.3	63.3	2.62
N7	3.819	3.819	30.846	76.1	58.1	3.28
N8	3.821	3.821	30.833	79.1	67.9	2.29

3 Results and Discussion

Figure 1 shows the XRD patterns of Na-doped samples in high contents. It is clear from the XRD analysis that all the samples are mainly composed of Bi-2212 although they have minor impurity phases such as Bi_2CaO_4 and $Bi_{0.75}Sr_{1.25}O_3$ (shown in Fig. 1 by *asterisk* and *circle*, respectively). On the other hand, any impurity phase with Na was not detected by XRD in all the samples, indicating that Na can entirely incorporate into the crystal structure of Bi-2212 phase. The lattice parameters for all the samples are shown in Table 1. It can be seen that the doping of Na for Cu causes changes in the lattice constants *a*, *b*, and *c*, indicating incorporate degree of Na in the crystal structure of the Bi-2212 phase. It is obvious that bond strengths between doped Na^+ element and oxygen within the CuO_2 planes can change because of Na^+ ions incorporated by Cu^{2+} ions in the crystallographic unit cell of Bi-2212. Note that the changing of *a* and *b* lattice constants depends on the changes of Cu-O bonding lengths on the CuO_2 planes, while the cell parameter *c* is generally associated with electrostatic forces between BiO-BiO layers which can be a repulsive or attractive force due to changing oxygen concentration in BiO layers.

On the other hand, the lattice *c* parameter of samples produced in this work spans between 30.807 and 30.883 Å, implying that over-Na doping does not create a major phase transition in crystallographic structure of samples.

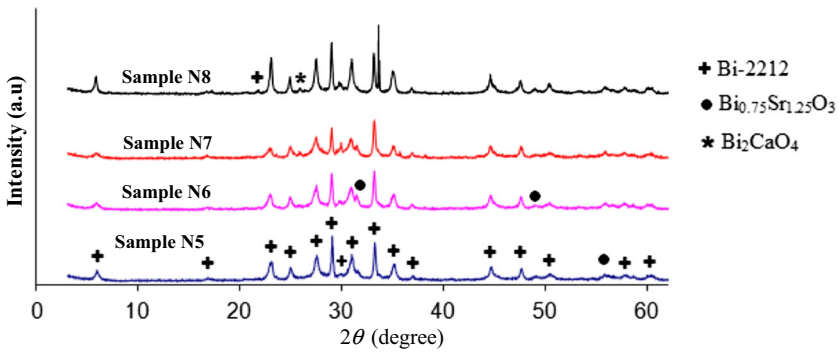

Fig. 1 XRD patterns of the N5, N6, N7, and N8 samples. The *symbols* indicate the different phases: *plus sign*, Bi-2212; *asterisk*, Bi_2CaO_4; *circle*, $Bi_{0.75}Sr_{1.25}O_3$

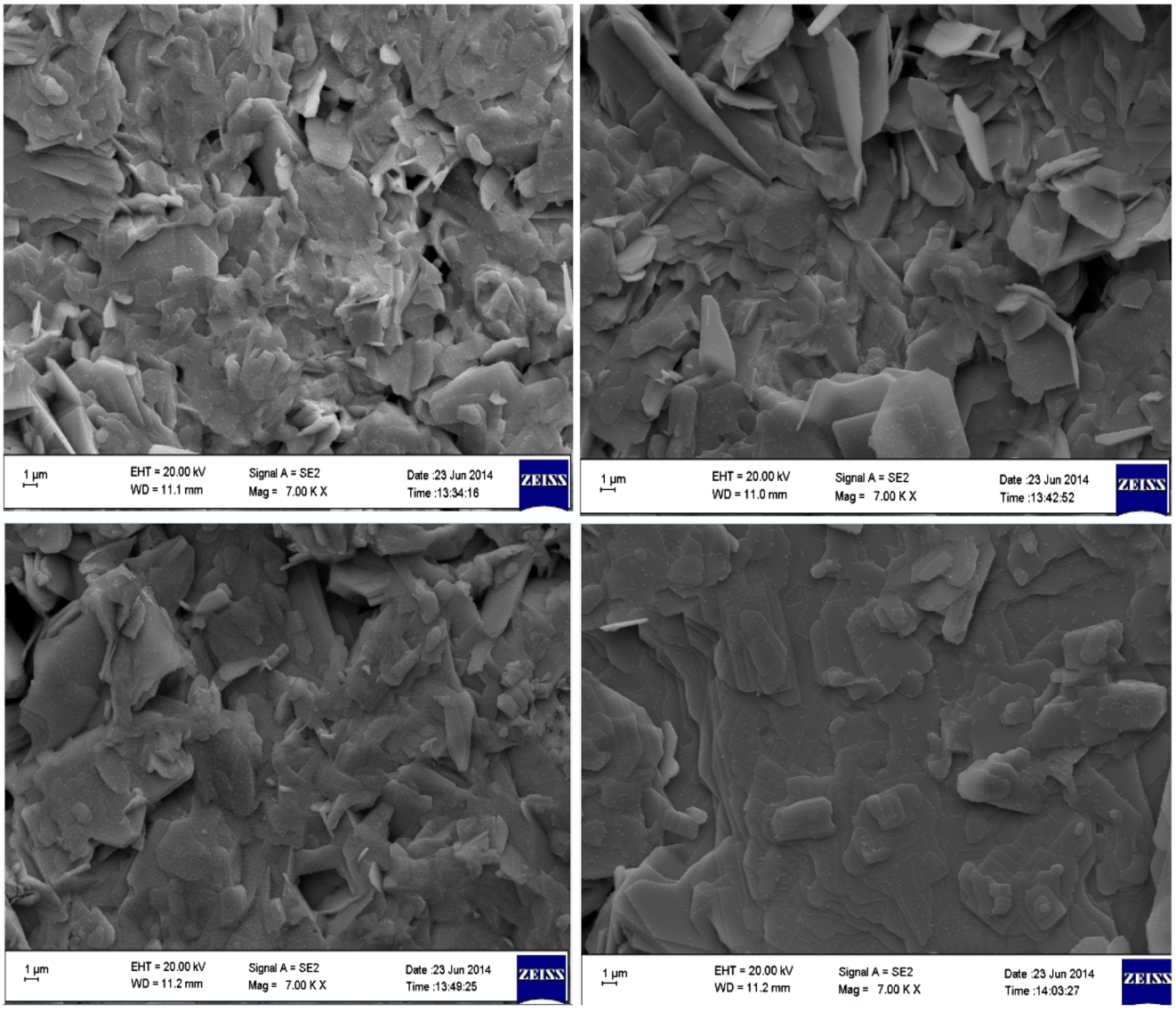

Fig. 2 SEM micrographs obtained in the surfaces of **a** N5,; N6,; N7,; and **d** N8 samples

Figure 2 shows surface micrographs for the N5, N6, N7, and N8 samples. It is clearly seen that the SEM images in sample N8 show better granular agglomeration and more flaky grains, showing strong links between them. It can be expected that voids occurred between grains in the structure of BSCCO ceramics have irregular shape and dimensions due to randomly oriented grains, which are basic characteristics of polycrystalline superconductors. However, sample N8 containing maximum Na in this work shows better homogeneity and more granular structure compared to other samples, which reflects the presence of better intergrain connectivity and less voids. In addition, one can see from the XRD figure that the peak intensities of sample N8 at peak values such as $2\theta \approx 5.7°$; 24.9°; 28.9° are greater than those of other samples, suggesting the improvements in grain sizes and better orientation of grains.

The degradation or improvement of crystallinity in BSCCO ceramics can be also interpreted by grain size of ceramic superconductors which can be easily calculated by the Debye-Scherrer equation. It is well known that BSCCO ceramics contain many randomly oriented plates or rod-like grains in their structure when they are prepared by solid-state reaction especially, implying many grain boundaries. Enhancements in grain sizes cause less grain boundaries, implying an improvement on the superconducting properties of system due to better alignment of grains and reduced voids.

According to Debye-Scherrer, in broadening region, the average size of a crystal is defined as follows [21]:

$$t = \frac{0.9\,\lambda}{B\,\cos\theta_B} \tag{1}$$

where t is the thickness of the crystal, λ is the wavelength, θ_B is the Bragg angle, and B is the line broadening, by reference to a standard, so

$$B^2 = B_m^2 - B_s^2 \tag{2}$$

where B_s is the half width of the standard material in radians.

The calculated grain thickness values for the N5, N6, N7, and N8 samples have been found to be about 50.7, 42.9, 41.4, and 66.85 nm, respectively. BSCCO ceramics can generally exhibit many impurity phases due to parameters such as the oxidation state and electronegativity of chemical doping element, the changes in annealing conditions during their preparation, and the purity rates of the used precursor materials, indicating that it is a very difficult task to reach the presence of strong links between the superconducting grains obtained from the large grain size. Thus, the obtained largest grain size (66.85 nm) for sample N8 is very important, since high Na doping for Cu site ensures a considerable improvement in the microstructural properties of Bi-2212 phase contrary to expectations.

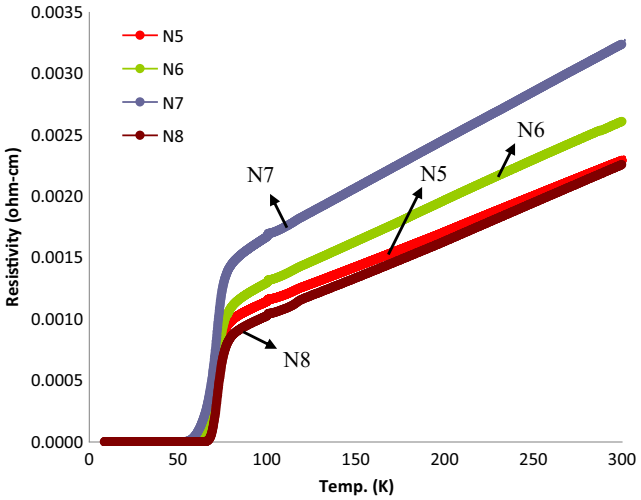

Fig. 3 Electrical resistivity as a function of temperature curves for all the samples

The variation of resistivity as a function of temperature for all samples is shown in Fig. 3. It is clear that the room temperature DC resistivity is the lowest for sample N8, suggesting that it has more suitable electric charge carrier density and better metallic behavior.

It is apparent from the figure that T_C^{onset} values above 75 K in all samples are responsible for dominant Bi-2212 phases, while the highest T_C^{offset} value for sample N8 depends on smooth grain orientation and improving grain morphology in terms of better coupling. The observed transition width in all samples is low, indicating that samples have only a small fraction of impurity phase. On the other hand, it was observed that sample N8 of $x = 0.5$ Na content increased the offset critical transition temperature from 62.1 to 67.9 K, in comparison with that of sample N5 including minimum Na content in this work, indicating that sample N8 has the best intergrain connectivity among all the studied samples.

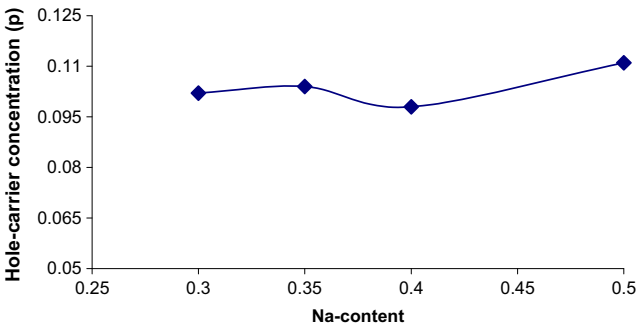

Fig. 4 Variation of hole-carrier concentration vs. Na content

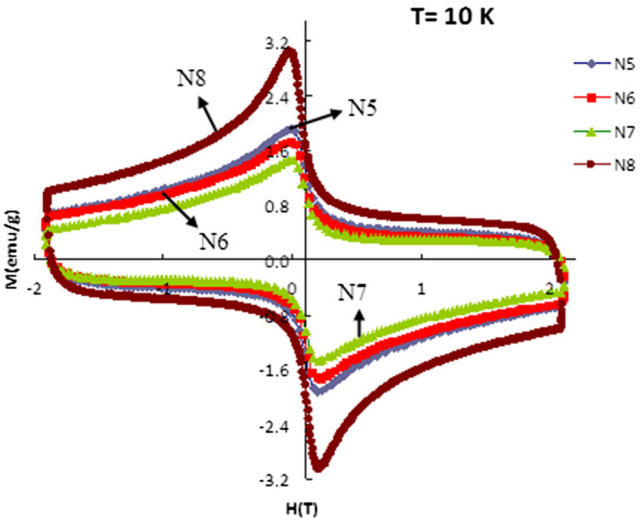

Fig. 5 Magnetization hysteresis curves for all samples measured at 10 K and ±2 T external applied magnetic field

The hole-carrier concentrations per Cu ion, P, are calculated by means of the following relation [22]:

$$p = 0.16 - \left[\left(1 - \frac{T_{\mathrm{C}}^{\mathrm{offset}}}{T_{\mathrm{C}}^{\mathrm{max}}}\right)/82.6\right]^{1/2} \tag{3}$$

where T_C^{max} is taken as 85 K for Bi-2212 phase [23, 24] and $T_{\mathrm{C}}^{\mathrm{offset}}$ values are those shown in Table 1. Figure 4 shows the variations of hole-carrier concentrations as a function of Na content. It is well known that the density of mobile holes in type II superconductors is closely associated with superconducting transition temperatures. It is obvious that sample N8 has the highest hole numbers when compared to other samples, indicating that the effective valency because of the incorporation of Cu^{+2} ions by Na^{+} ions increases.

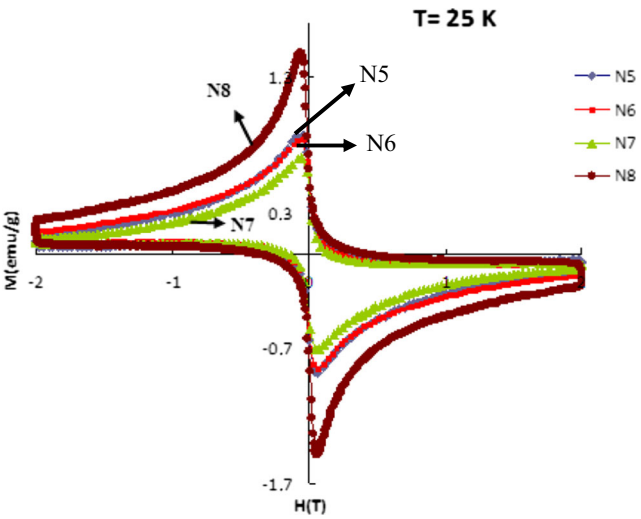

Fig. 6 Magnetization hysteresis curves for all samples measured at 25 K and ±2 T external applied magnetic field

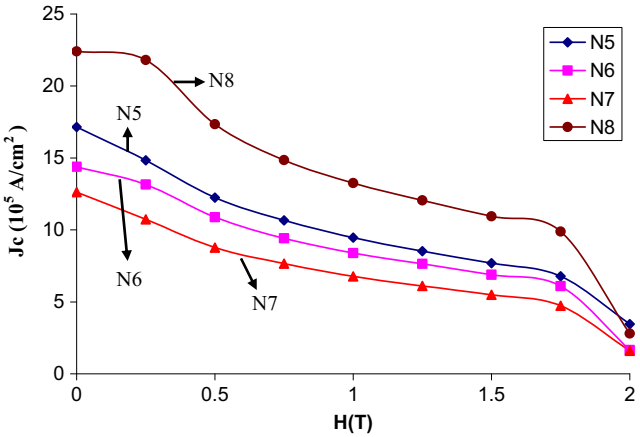

Fig. 7 Calculated critical current densities for all the samples at 10 K as a function of applied field

The magnetic hysteresis cycles, between applied fields of ±2 T, for all the samples, at 10 and 25 K, are presented in Figs. 5 and 6, respectively. All the samples show characteristic diamagnetic behavior of type II superconductors with similar magnetization hysteresis loops even if they have different values with respect to M_{R} (remnant magnetization) and H_{c} (coercive field). It is obvious that the width of hysteresis loops for sample N8 at both 10 and 25 K temperatures is larger than that of other samples, implying the formation of new pinning centers in addition to better interconnectivity of the grains along with reduced grain boundaries due to large grains.

From these data, the J_{c} values of the samples were determined using Bean's model [25]:

$$\mathrm{J_c} = 30\frac{\Delta M}{d}, \tag{4}$$

where J_{c} is the magnetization current density in amperes per square centimeter of a sample. $\Delta M = M_{+} - M_{-}$ is measured in electromagnetic units per cubic centimeter, and d is the thickness of sample.

Figure 7 shows the calculated critical current densities for all the samples, as a function of the applied magnetic field, at 10 K. The increase in J_{c} values for BSCCO ceramics is generally based on the enhancement of flux pinning introduced by the doping of foreign elements. The evidence of such developments is that the width ΔM of the hysteresis loop in BSCCO samples contained the new effective pinning centers by the doping of impurities is two–three times bigger than that of undoped pure BSCCO sample. As can be seen in Fig. 7, the value of critical current density in sample N8 at all applied magnetic fields is larger than that of sample N5. This result suggests that sample

N8 has the new occurred pinning centers in addition to important parameters such as better intergranular connectivity between grains and the reduction of the number of grain boundaries as clearly proved from XRD and SEM figures.

4 Conclusions

In this study, $Bi_2Sr_2Ca_1Cu_{2-x}Na_xO_y$ ceramics including Na content in range of $x = 0.3-0.5$ were synthesized by solid-state reaction method. X-ray diffraction analysis (XRD), scanning electron microscopy (SEM), DC electrical resistivity, and magnetic hysteresis loop measurements were used to investigate the effects of overNa doping on superconducting properties of Bi-2212 system. The results indicate that all the samples have the basic characteristic features of the Bi-2212 phase.

On the other hand, XRD measurements show that dominant phase in all samples is Bi-2212 together with a small amount of impurity phases. The crystallinity in sample N8 improves significantly. SEM micrographs reveal that the grain size for sample N8 increases, implying less porosity and better conductivity between grains. The maximum grain size of 66.85 nm is obtained for sample N8. The area enclosed by the magnetization curve for sample N8 significantly increases, implying the highest J_c values among other samples.

Acknowledgments All samples have been prepared in the MEİTAM Central Laboratory in Mersin University in Turkey. Both SEM and XRD measurements have been made in the MEİTAM Central Laboratory in Mersin University; the other measurements in this study have been made in the METU Central Laboratory in Middle East Technical University in Ankara in Turkey. On the other hand, I wish to thank M.Sc. Aynur Gurbüz and PhD. M. Serkan Yalçin in the MEİTAM Central Laboratory and Dr. Ibrahim Çam in the METU Central Laboratory for their experimental support and very meticulous work.

References

1. Bilgili, O., Selamet, Y., Kocabas, K.: J. Supercond. Nov. Magn. **21**, 439 (2008)
2. Sozeri, H., Ghazanfari, N., Ozkan, H., Kılıc, A.: Supercond. Sci. Technol. **20**, 522 (2007)
3. Sotelo, A., Mora, M., Madre, M.A., Diez, J.C., Angurel, L.A., de la Fuente, G.F.: J. Eur.Ceram. Soc. **25**, 2947 (2005)
4. Jiang, L., Sun, Y., Wan, X., Wang, K., Xu, G., Chen, X., Ruan, K., Du, J.: Physica C **300**, 61 (1998)
5. Zargar Shoushtari, M., Mousavi Ghahfarokhi, S.E.: J. Supercond. Nov. Magn. **24**, 1505 (2011)
6. Abou-Aly, A.I., Abdel Gawad, M.M.H., Awad, R., G-Eldeen, I.: J. Supercond. Nov.Magn. **24**, 2077 (2011)
7. Sotelo, A., Amaveda, H., Madre, M.A., Diez, J.C., Angurel, L.A., de la Fuente, G.F.: Bol. Soc. Esp. Ceram. Vidr. **44**, 199 (2005)
8. Şakiroğlu, S., Kocabaş, K.: J. Supercond. Nov. Magn. **24**, 1321 (2011)
9. Khalil, S.M.: J. Phys. Chem. Solids **62**, 457 (2001)
10. Sotelo, A., Madre, M.A., Diez, J.C., Rasekh, Sh., Angurel, L.A., Martinez, E.: Supercond. Sci. Technol. **22**, 034012 (2009)
11. Madre, M.A., Amaveda, H., Mora, M., Sotelo, A., Angurel, L.A., Diez, J.C.: Bol. Soc.Esp. Ceram **47**, 148 (2008)
12. Chen, Y.L., Stevens, R.: J. Am. Ceram. Soc **75**, 1150 (1992)
13. Ramesh, R., Green, S., Jiang, C., Mei, Y., Rudee, M., Luo, H., Thomas, G.: Phys. Rev. B: Condens. Matter **38**, 7070 (1988)
14. Agail, A., Abd-Shukor, R. J. Mater. Sci. **27**, 1273 (2014)
15. Albiss, B.A., Obaidat, I.M., Gharaibeh, M., Ghamlouche, H., Obeidat, S.M.: Solid State Commun **150**, 1542 (2010)
16. Ma, R.C., Song, W.H., Zhu, X.B., Zhang, L., Liu, S.M., Fang, J., Du, J.J., Sun, Y.P., Li, C.S., Yu, Z.M., Feng, Y., Zhang, P.X.: Physica C **405**, 34 (2004)
17. Ozkurt, B.: J. Alloys Comp **579**, 132 (2013)
18. Ozkurt, B.: J. Mater. Sci.: Mater. Electron. **24**, 2426 (2013)
19. Ozkurt, B.: J. Mater. Sci.: Mater. Electron. **25**, 3295 (2014)
20. Ozkurt, B.: J. Supercond. Nov. Magn. (2014). doi:10.1007/s10948-014-2623-z
21. Yıldırım, G., Bal, S., Yücel, E., Dogruer, M., Akdoğan, M., Varilci, A., Terzioğlu, C.: J. Supercond. Nov. Magn. **25**, 381 (2012)
22. Azzouz, B.F., Mchirgui, A., Yangui, B., Boulesteix, C., Salem, B.M.: Physica C **356**, 83 (2001)
23. Kucukomeroglu, T., Bacaksız, E., Terzioglu, C., Varilci, A.: Thin Solid Films **516**, 2913 (2008)
24. Bal, S., Dogruer, M., Yildirim, G., Varilci, A., Terzioglu, C., Zalaoglu, Y.: J. Supercond. Nov. Magn. **25**, 847 (2012)
25. Bean, C.P.: Phys. Rev. Lett **8**, 250 (1962)